

Jørgen Lauritzen Jensen

Quasi-non-linear fracture mechanics analysis of splitting failure in moment-resisting dowel joints

Received: July 26, 2004 / Accepted: January 13, 2005

Abstract This article addresses the splitting failure of moment-resisting dowel-type fastener joints, in which the failure may be attributed to the perpendicular-to-grain loading of one single dowel located close to the end of a beam. A quasi-non-linear fracture mechanics model based on beam on elastic foundation theory is applied. A simple approximation suitable for practical design is also proposed. Model predictions of the influence of edge distances and end distances are compared with test results.

Key words Moment-resisting dowel joints · Perpendicular-to-grain load · Splitting · Quasi-non-linear fracture mechanics · Beam on elastic foundation

Introduction

Dowel-type fastener joints fail either in a ductile manner, characterized by bending of the fastener and/or embedment of the fastener into the wood, or in a brittle manner, characterized by splitting of the wood. The ductile failure modes are fairly well understood. Widely accepted design expressions have been derived for individual fasteners based on theory of plasticity,^{1,2} and also the strength and stiffness of moment-resisting joints can be reliably predicted.^{3,4} Research on the brittle splitting failure modes is still at an early stage. The splitting failure mode of centrally loaded joints has only recently been studied analytically,^{5–9} and none of the developed models have yet won wide acceptance. Theoretical attempts to address the splitting failure modes of moment-resisting joints do not appear to have been reported.

The present article addresses the splitting failure of the simplest possible moment-resisting dowel-type fastener

joint, in which the failure is attributed to the perpendicular-to-grain loading of one single dowel located close to the end of a beam. Beam on elastic foundation (BEF) theory for a Timoshenko beam is used, and fracture mechanics is introduced through the constitutive relations for the foundation. The stiffness of the foundation is chosen so that the perpendicular-to-grain tensile strength and fracture energy properties are correctly represented. This particular choice of foundation stiffness makes a conventional maximum stress failure criterion lead to the same solution as the fracture mechanics compliance method.

Theory

Figure 1 shows schematically the type of joint considered, its geometry, and assumed failure mode. The encircled part in Fig. 1 is assumed to behave as a beam on elastic foundation (BEF), the part above the crack being the beam (edge distance, h_e , being beam depth), and the part beneath the crack serving as the foundation. BEF theory may be expected to be suitable for application to the problem considered here because h_e in moment-resisting joints is usually small as compared with the total beam depth, h . The end distance (distance from the critical dowel where splitting failure initiates to the beam end) is denoted s .

The geometry, loading, and boundary conditions for the beam on elastic foundation are shown in Fig. 2. Note that P is the load on the critical dowel.

The deflection of the beam axis at the loading point is denoted as $w(s)$. The foundation stress at the loading point is denoted as $\sigma(s)$, and is given by

$$\sigma(s) = Kw(s) \quad (1)$$

where K is the foundation stiffness (units: N/m³).

The deflection at the loading point may in general be expressed as

$$w(s) = \frac{P}{EI} \Psi(s) \quad (2)$$

J.L. Jensen (✉)
Institute of Wood Technology, Akita Prefectural University,
11-1 Kaiezaka, Noshiro 016-0876, Japan
Tel. +81-185-52-6985; Fax +81-185-52-6976
e-mail: jensen@iwt.akita-pu.ac.jp

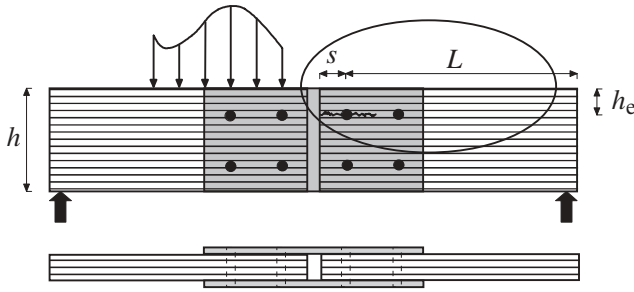


Fig. 1. Definition of geometrical parameters

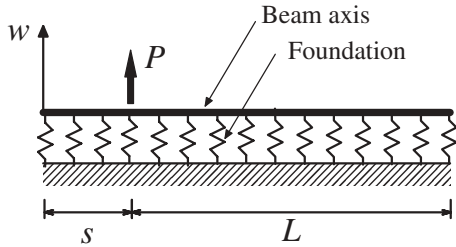


Fig. 2. Beam on elastic foundation model. Geometry, loading, and boundary conditions

E being the modulus of elasticity in the grain direction and I the moment of inertia of the beam on elastic foundation.

Assuming that the maximum foundation stress occurs at the loading point, and that failure occurs when the maximum foundation stress reaches the perpendicular-to-grain tensile strength of the wood, f_t , the failure load, P_c , thus becomes

$$P_c = f_t \frac{EI}{K} \frac{1}{\Psi(s)} \quad (3)$$

The parameters λ and η are defined as

$$\lambda = \frac{Kb}{EI}, \quad \eta = \frac{Kb}{GA_s} \quad (4)$$

where b is beam width, $I = bh_c^3/12$, $A_s = 5bh_c/6$ (rectangular cross section, beam depth h_c), and G is shear modulus.

The solution to the governing differential equations for a Timoshenko beam on elastic foundation divides into two solutions depending on λ and η . By means of solutions given by Pilkey,¹⁰ the function $\Psi(s)$ may for $L \rightarrow \infty$ be written

$$\lambda \geq \frac{1}{4}\eta^2:$$

$$v^2 = \frac{1}{2}\sqrt{\lambda} + \frac{1}{4}\eta, \quad u^2 = \frac{1}{2}\sqrt{\lambda} - \frac{1}{4}\eta$$

$$\Psi(s) = \frac{v^4 \sin^2 us + uv(u^2 - 3v^2) \cos us \sin us + u^2 v^2 \left(3 \cos^2 us - \frac{1}{2} + \frac{3}{2} e^{2vs} \right) + u^4 \left(\frac{1}{2} - \frac{1}{2} e^{2vs} \right)}{2u^2 v (u^2 + v^2)^2 e^{2vs}} \quad (5a)$$

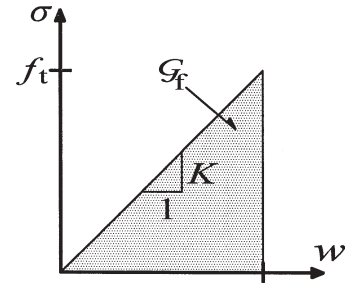


Fig. 3. Constitutive relation for the foundation

$$\lambda < \frac{1}{4}\eta^2:$$

$$v^2 = \frac{1}{2}\eta + \sqrt{\frac{1}{4}\eta^2 - \lambda}, \quad u^2 = \frac{1}{2}\eta - \sqrt{\frac{1}{4}\eta^2 - \lambda}$$

$$\Psi(s) = \frac{(v-u)^4 + 3uv(v-u)^2 + uv \left(\frac{v}{e^{vs}} - \frac{u}{e^{us}} \right)^2 + \left(\frac{v^2}{e^{vs}} - \frac{u^2}{e^{us}} \right)^2}{2u^2 v^2 (v-u)^2 (v+u)} \quad (5b)$$

Equation 5 is based on the assumption that $L \rightarrow \infty$. This assumption does, however, not impose any practical limitations on the model considered here. Previous analyses of beams on elastic foundations show that no significant error is introduced by assuming $L \rightarrow \infty$ if $L > 10h_c$.

Foundation properties

The damage and fracture performance of wood is in general non linear, but is in the present analysis represented by a linear response that is equivalent in terms of peak stress, f_t , and fracture energy dissipation, G_f , as indicated in Fig. 3.

The fracture energy of the foundation is in general given as

$$G_f = \int_0^\infty \sigma dw \quad (6)$$

and for the linear response shown in Fig. 3 it follows that the stiffness of the foundation, K , is given by

$$K = \frac{f_t^2}{2G_f} \quad (7)$$

The present strength analysis of mode I failure using BEF theory and introducing fracture mechanics through the linearized constitutive relation as given by Eq. 7 is a

complete analogy to the fracture mechanics application of the Volkersen model to strength analysis of mode II failure in lap joints.¹¹ The analysis has been termed quasi-non-linear fracture mechanics because the material responses are assumed to be linear as in linear elastic fracture mechanics (LEFM), but at the same time the tensile strength is assigned a finite value, not an infinite value as in LEFM, and the finite, nonzero size of the fracture region is considered, leading to a failure load, which is not proportional to the square root of the fracture energy. It has previously been shown^{12–14} that assigning the foundation the stiffness as given by Eq. 7 makes the above-derived solution, which is based on a usual maximum stress failure criterion, lead to the same solution as obtained by using the compliance method of fracture mechanics.

Two important special cases of Eqs. 3–5 may be identified, namely $s = 0$ and $s \rightarrow \infty$. In both cases, the two solutions (Eqs. 5a and 5b) merge into just one solution, which by use of Eq. 7 becomes

$$P_c = \gamma P_0$$

$$P_0 = 2bC_1\sqrt{h_c}, \quad C_1 = \sqrt{\frac{5}{3}GG_f}$$

$$\gamma \rightarrow \begin{cases} \frac{1}{2\sqrt{2\zeta+1}} & \text{for } s = 0 \\ \frac{\sqrt{2\zeta+1}}{\zeta+1} & \text{for } s \rightarrow \infty \end{cases} \quad (8)$$

$$\zeta = \frac{C_1}{f_t} \sqrt{10 \frac{G}{E} \frac{1}{h_c}}$$

Equation 8 is in agreement with the previously developed solutions for glued-in rod joints subjected to pure shear load¹² and dowels loaded perpendicular to grain.¹⁴ From Eq. 8 it follows

$$P_{c,0} = \frac{1}{2} \frac{\zeta+1}{2\zeta+1} P_{c,\infty} \quad (9)$$

where $P_{c,0}$ is the failure load for $s = 0$ and $P_{c,\infty}$ is the failure load for $s \rightarrow \infty$. The fact that $P_{c,0} < \frac{1}{2} P_{c,\infty}$ for finite values of f_t is due to the different boundary conditions for the two situations; for $s = 0$ the beam end can rotate freely, while for $s \rightarrow \infty$ the rotation of the beam end is zero.

Results from LEFM are obtained by letting $f_t \rightarrow \infty$. In Eq. 8, this leads to

$$P_{c,0} = \frac{1}{2} P_{c,\infty} = b(G\Gamma_f h_c / 0.6)^{\frac{1}{2}}$$

The LEFM solution obtained here for $s \rightarrow \infty$ is the same as that obtained by different LEFM approaches^{6,8,15} if the edge distance in the latter is small as compared with the total beam depth, and it is also the same solution as given by another simple LEFM approach⁷ if in the latter the shear area $A_s = 5bh_c/6$ is used instead of the area $A = bh_c$.

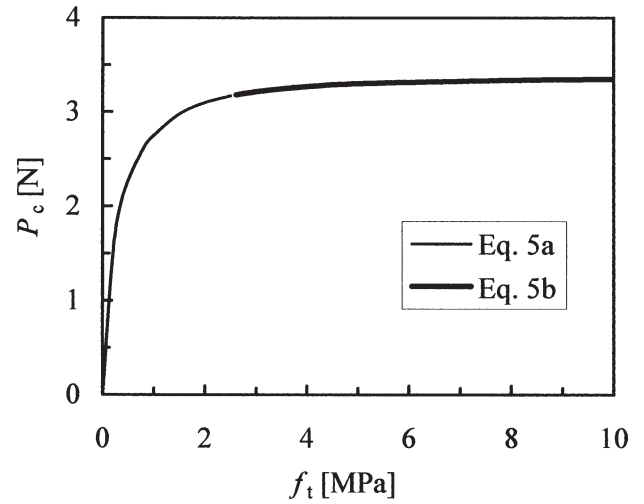


Fig. 4. Influence of perpendicular-to-grain tensile strength (f_t) on failure load (P_c)

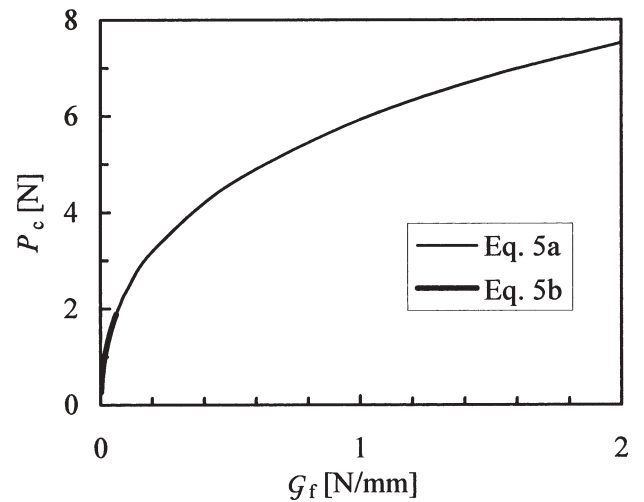


Fig. 5. Influence of fracture energy (G_f) on failure load (P_c)

In Figs. 4 and 5 are shown examples of the influence of perpendicular-to-grain tensile strength, f_t , and fracture energy, G_f . The examples shown use the following properties: $b = 25$ mm, $h_c = 40$ mm, $s = 160$ mm, $E = 7200$ MPa, $G = 400$ MPa; in Fig. 4 $G_f = 0.17$ N/mm, and in Fig. 5 $f_t = 1.5$ MPa. While the failure load asymptotically approaches an upper limit for $f_t \rightarrow \infty$, there is no upper limit for $G_f \rightarrow \infty$.

It may also be noticed that the present theory predicts a very modest influence of the modulus of elasticity (MOE), while the shear modulus has a significant impact on the failure load. As easily seen from Eq. 8, the failure load asymptotically approaches an upper limit for $E \rightarrow \infty$, while there is no upper limit for $G \rightarrow \infty$.

Materials and methods

All specimens were made of glulam of Japanese cedar (*Cryptomeria japonica*), width, $b = 25$ mm. The laminae

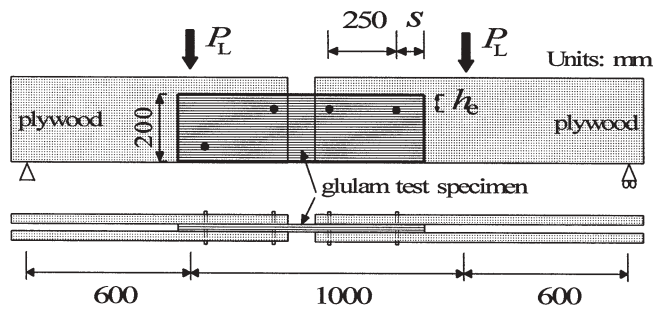


Fig. 6. Test setup and geometry of specimens

(thickness 26 mm) were all the same grade and were without finger joints. MOE in the grain direction was determined by measuring the longitudinal vibration frequency of the glulam beams, from which the specimens were cut. All tests were displacement controlled and failure occurred after 2–3 min.

The symmetrical three-member joints, with the glulam test specimen as the middle member and 25-mm plywood plates as side members, were subjected to a pure moment in a four-point bending test setup as shown in Fig. 6, causing splitting failure at the rightmost dowel (edge distance h_e , and end distance s). Dowels with diameters of 14 mm were used in 15-mm holes, and a gap was deliberately made between middle and side members to assure no transfer of forces due to friction.

Nine different combinations of h_e and s were tested: For $h_e = 20$ mm and for $h_e = 40$ mm, $s = 20, 40, 80$, and 160 mm were tested, and for $h_e = 60$ mm, $s = 40$ mm was tested. Twelve specimens were prepared for each condition. However, only specimens without knots in the vicinity of the point of crack initiation were selected in order to limit the variation, resulting in 7–12 specimens tested for each condition. Moisture content (MC) was 14%, density was 372 kg/m³ at the given MC, and MOE was 7200 MPa.

The load, P , acting perpendicular to grain on the critical dowel is calculated as

$$P = 2.4P_L + P_{sw} \quad (10)$$

where $2P_L$ is the total load applied by the testing machine and $P_{sw} \approx 160$ N is the contribution from the weight of the plywood.

Tests were also conducted on double cantilever beam (DCB) specimens (Fig. 7a) to determine the fracture energy of the glulam, and on plate joint specimens (Fig. 7b) to determine the tensile strength. Eleven knot-free DCB specimens, $b = 25$ mm, $h = 40$ mm, $a = 250$ mm, and $L = 550$ mm, were tested. Plate joints were tested using two different edge distances: $h_e = 20$ mm and 40 mm. Ten to 12 knot-free specimens with $b = 25$ mm, $h = 210$ mm, and $L = 500$ mm were tested for each h_e value.

Results and discussion

The model derived in the present article requires two fracture properties, fracture energy G_f and perpendicular-

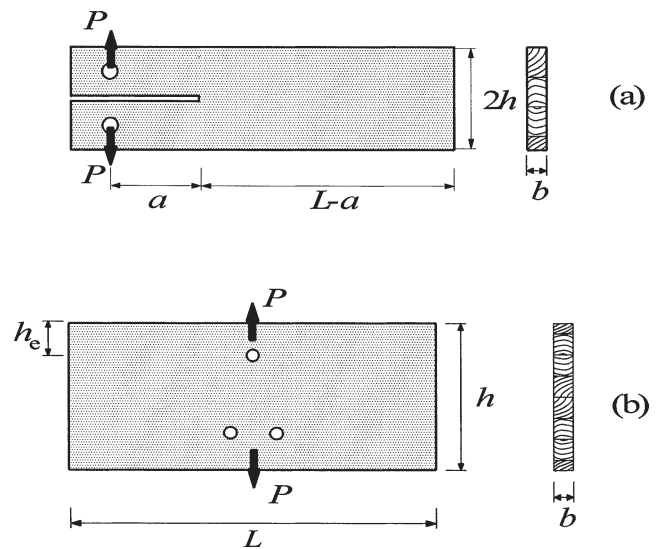


Fig. 7. Double cantilever beam specimen for determination of fracture energy (a) and plate joint specimen for determination of perpendicular-to-grain tensile strength (b)

to-grain tensile strength f_t , as input parameters. Because f_t is highly volume dependent, it is not obvious what volume (or cross-sectional area) should be used if attempting to determine it directly by tension tests. In the following, f_t is therefore determined by means of the plate joint specimen.

Analyses of the DCB and plate joint specimens based on the same BEF and fracture mechanics theory as given in this article have been presented elsewhere.^{13,14} These models likewise both depend on G_f and f_t , and an iterative process of successive calculations is necessary (two to three calculations) to derive G_f and f_t . The results obtained were $G_f = 0.21$ N/mm and $f_t = 1.05$ MPa, where f_t is the mean value obtained from plate joint specimens with $h_e = 20$ mm ($f_t = 1.29$ MPa) and 40 mm ($f_t = 0.81$ MPa).

The fracture energy may also be determined from the DCB specimen tests using a simple linear elastic fracture mechanics solution,⁷ which does not depend on f_t , resulting in $G_f = 0.17$ N/mm. In that case the plate joint tests¹⁴ result in $f_t = 1.64$ MPa (mean of 1.22 MPa and 2.05 MPa obtained for $h_e = 40$ mm and $h_e = 20$ mm, respectively). In the following $(f_t, G_f) = (1.05$ MPa, 0.21 N/mm) is used, but $(f_t, G_f) = (1.64$ MPa, 0.17 N/mm) also leads to good predictions. The fact that significantly different values of f_t are obtained for $h_e = 20$ mm and 40 mm questions the suitability of using the plate joint specimen for deriving f_t . Further discussions on this problem may be found elsewhere.^{13,14}

Figure 8 shows the results of the tests on moment-resisting joints compared with the predictions as given by Eq. 5a. The theoretical model predicts amazingly well the influence of edge distance, h_e , and end distance, s .

Figure 8 indicates that a bilinear approximation may be suitable for a simplification of Eq. 5a. Equation 8 gives the point for $s = 0$ and the horizontal upper limit. Using the tangent at $s = 0$ leads to the simple expression

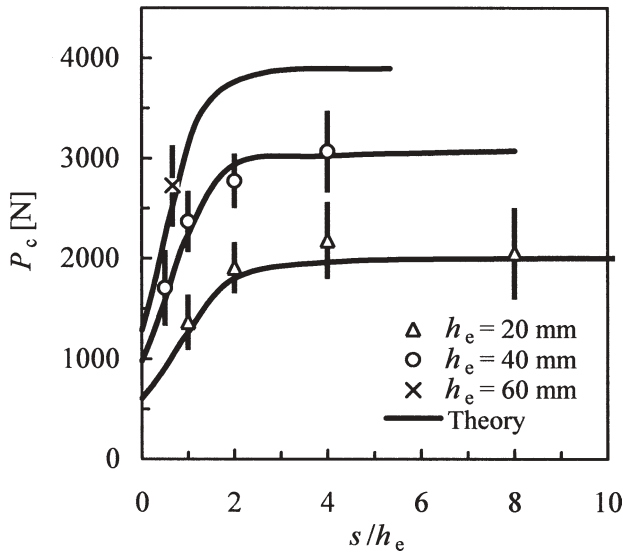


Fig. 8. Equation 5a compared with experimental failure loads. $f_t = 1.05$ MPa, $G_t = 0.21$ N/mm, bars indicate standard deviation

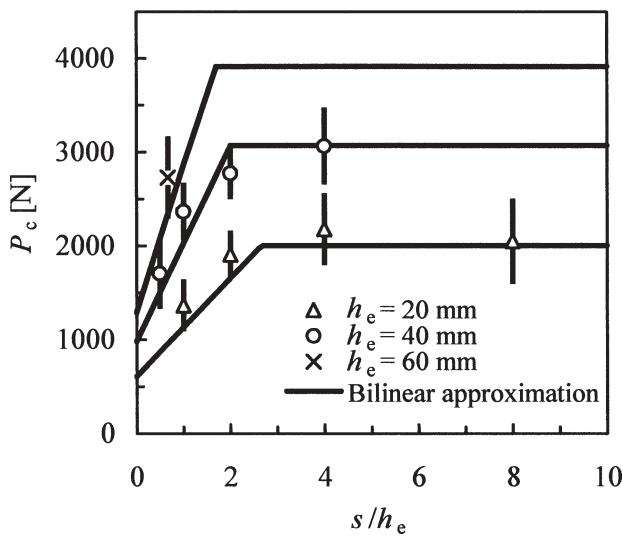


Fig. 9. Equation 11a compared with experimental failure loads. $f_t = 1.05$ MPa, $G_t = 0.21$ N/mm, bars indicate standard deviation

$$\frac{P_c}{P_0} = \min \left\{ \begin{array}{l} \frac{1}{2\sqrt{2\zeta+1}} + bf_t s \\ \frac{\sqrt{2\zeta+1}}{\zeta+1} \end{array} \right. \quad (11a)$$

$$P_0 = 2bC_1\sqrt{h_e}, \quad \zeta = \frac{C_1}{f_t} \sqrt{10 \frac{G}{E} \frac{1}{h_e}}, \quad C_1 = \sqrt{\frac{5}{3} GG_t}$$

Equation 11a is shown together with the test results in Fig. 9. Judging from Fig. 9, the bilinear relation given by Eq. 11a seems in general to give a slightly conservative (as compared with Eq. 5a) but fairly good approximation, and may be worth considering as a simple design tool. While the

solutions given by Eqs. 5a and 5b are each numerically restricted to cover certain combinations of some geometrical and material properties, Eq. 11a contains no such restrictions and may, without numerical problems, be used for any finite geometrical and material properties.

Although Eq. 11a leads to very good predictions for the joints reported in the present article, it still remains to be investigated whether it holds for other conditions as well.

Conclusions

A quasi-non-linear fracture mechanics model based on BEF theory was applied for the analysis of splitting failure in moment-resisting dowel joints. An approximation simple enough for practical design was also proposed.

Tests were conducted on simple moment-resisting joints with only two dowels, and end distance and edge distance of the critical dowel were varied. Although theoretical predictions were in excellent agreement with test results, indicating that the theoretical approach is basically sound, further testing is needed on more realistic dowel configurations.

The models presented depend on the perpendicular-to-grain tensile strength. The tensile strength is highly volume dependent, and it is difficult to determine it directly by tension tests because the appropriate volume (or cross-sectional area) of the test specimen is not obvious. In the present article, so-called plate joint specimens were used for estimation of the tensile strength. More investigations are needed to reveal whether the plate joint specimen is suitable as a standard test specimen for that purpose or if another way of deriving an appropriate value of the perpendicular-to-grain tensile strength is needed.

References

- Johansen KW (1941) Forsøg med træforbindelser. Bygningsstatistiske Meddelelser, årgang XII
- Larsen HJ (1979) Design of bolted joints. In: Proceedings of the International Council for Research and Innovation in Building and Construction, CIB-W18 Meeting Twelve, Bordeaux, France, paper No. 12-7-2
- Foschi RO (1977) Analysis of wood diaphragms and trusses. Part II. Truss-plate connections. Can J Civ Eng 4:353-362
- Jensen JL, Larsen HJ (1998) Modelling of semi-rigid joints and their influence on the behaviour of structures. In: Natterer J, Sandoz JL (eds) Proceedings of the 5th World Conference on Timber Engineering, Montreux, Switzerland, Vol 1, pp 305-312
- Jorissen AJM (1998) Double shear timber connections with dowel-type fasteners. Ph.D. thesis, Delft University Press, Delft, The Netherlands
- van der Put TACM, Leijten AJM (2000) Evaluation of perpendicular-to-grain failure of beams caused by concentrated loads of joints. In: Proceedings of the International Council for Research and Innovation in Building and Construction, CIB-W18 Meeting Thirty-three, Delft, The Netherlands, paper No. 33-7-7
- Larsen HJ, Gustafsson PJ (2001) Dowel joints loaded perpendicular to grain. In: Proceedings of the International Council for Research and Innovation in Building and Construction, CIB-W18 Meeting Thirty-four, Venice, Italy, paper No. 34-7-3

8. Jensen JL (2003) Splitting strength of beams loaded by connections. In: Proceedings of the International Council for Research and Innovation in Building and Construction, CIB-W18 Meeting Thirty-six, Colorado, USA, paper No. 36-7-8
9. Jensen JL, Gustafsson PJ, Larsen HJ (2003) A tensile fracture model for joints with rods or dowels loaded perpendicular-to-grain. In: Proceedings of the International Council for Research and Innovation in Building and Construction, CIB-W18 Meeting Thirty-six, Colorado, USA, paper No. 36-7-9
10. Pilkey WD (1994) Formulas for stress, strain, and structural matrices. Wiley, New York, pp 534–545
11. Gustafsson PJ (1987) Analysis of generalized Volkersen joints in terms of non-linear fracture mechanics. In: Verchery G, Cardon AH (eds): Mechanical behaviour of adhesive joints. Pluralis, Paris, pp 323–338
12. Jensen JL, Gustafsson PJ (2004) Shear strength of beam splice joints with glued-in rods. *J Wood Sci* 50:123–129
13. Jensen JL (2005) Quasi-non-linear fracture mechanics analysis of the double cantilever beam specimen. *J Wood Sci* 51:566–571
14. Jensen JL (2005) Quasi-non-linear fracture mechanics analysis of the splitting failure of single dowel joints loaded perpendicular to grain. *J Wood Sci* 51:559–565
15. Jensen JL (2005) Splitting strength of beams loaded perpendicular to grain by dowel joints. *J Wood Sci* 51:480–485